Agricultural Water Management 217 (2019) 303–315

Contents lists available at ScienceDirect

Agricultural Water Management

journal homepage: www.elsevier.com/locate/agwat

Evapotranspiration evaluation models based on machine learning algorithms—A comparative study

Francesco Granata

Department of Civil and Mechanical Engineering, University of Cassino and Southern Lazio, via G. Di Biasio 43, 03043 Cassino, FR, Italy

ARTICLE INFO

Keywords:
Actual evapotranspiration
Machine learning
Regression tree
Ensemble methods
Support vector regression
Irrigation

ABSTRACT

The constant need to increase agricultural production, together with the more and more frequent drought events in many areas of the world, requires a more careful assessment of irrigation needs and, therefore, a more accurate estimation of actual evapotranspiration. In recent years, several water management issues have been addressed by means of models derived from Artificial Intelligence research. When using machine learning based models, the main challenging aspects are represented by the choice of the best possible algorithm, the choice of adequately representative variables and the availability of appropriate data sets.

Machine learning algorithms may be a powerful tool for the prediction of actual evapotranspiration, when a time series of few years is available. Starting from the measurements of a sufficient number of climatic parameters it is possible to obtain forecasting models characterized by very high accuracy and precision. Three different evapotranspiration models have been compared in this study. The models differ in the input variables. Four variants of each model were applied, varying the machine learning algorithm: M5P Regression Tree, Bagging, Random Forest and Support Vector Regression. The data refers to an experimental site in Central Florida, characterized by humid subtropical climate.

The best outcomes have been provided by Model 1, whose input variables were net solar radiation, sensible-heat flux, moisture content of the soil, wind speed, mean relative humidity and mean temperature. Model 3, built from data only of mean temperature, mean relative humidity and net solar radiation, has provided still satisfactory results. Model 2, which adds the wind speed to the input variables of Model 3, has provided results that are absolutely comparable to those of Model 3 itself.

1. Introduction

The progressive increase in the world population continuously requires increases in agricultural production. Agriculture is the anthropic activity that consumes most water. The frequent events of drought affecting vast areas of the globe impose a more and more careful management of water resources both on a global scale and on the scale of the individual watersheds. A careful estimate of all the components of the water balance, in particular of evapotranspiration, is essential for a careful planning of irrigation practice.

Evapotranspiration is the combination of two separate processes whereby water is lost on the one hand from the soil surface by evaporation and on the other hand from the crop by transpiration (Jensen et al., 2016). Evaporation turns liquid water into water vapour, which is removed from the evaporating surfaces: generally, lakes, rivers, soils and wet vegetation. The energy required for the conversion process is provided by solar radiation and air temperature. Vapour pressure deficit and wind speed enhance the diffusion of water vapour in the atmosphere. Therefore, solar radiation, air temperature, air humidity and wind speed are climatological parameters that mainly affect the evaporation process.

Transpiration is the process by which the liquid water contained in plant organisms is vaporized and lost through the small stomatal openings on the leaves. Transpiration, as well as direct evaporation, depends on radiation, air temperature, air humidity and wind speed. Moreover, transpiration is highly depending on crop characteristics and agricultural practices.

Evaporation and transpiration are two simultaneous and almost indistinguishable processes (Kool et al., 2014). An assessment that does not consider the factors characterizing the crops can be done by introducing the concept of reference evapotranspiration (Jensen, 1968; Doorenbos and Pruitt, 1977), that is generally denoted as ET_0. Reference evapotranspiration is a climatic parameter and therefore depends only on climatic variables. Actual evapotranspiration ET_a can be evaluated from reference evapotranspiration by means of crop coefficients.

E-mail address: f.granata@unicas.it.

https://doi.org/10.1016/j.agwat.2019.03.015
Received 22 August 2018; Received in revised form 14 January 2019; Accepted 5 March 2019
Available online 12 March 2019
0378-3774/

Jensen et al. (2016) outlined the evolution of evapotranspiration estimating methods over the past century. Many evapotranspiration estimation models are empirical models based on statistical correlations of evapotranspiration with meteorological parameters (Abtew and Melesse, 2013). Performance may significantly depend on the location. Local recalibration may be needed. The simplest models are based on temperature only. The most popular empirical method, the Hargreaves-Samani equation, depends on both temperature and solar radiation (Hargreaves and Samani, 1982). More complex are energy balance methods, requiring knowledge of latent and sensible-heat flux.

The Penman–Monteith (P–M) equation could be considered as a physically based evapotranspiration model (Jensen et al., 2016). It is complete in describing the evapotranspiration because it takes into account moisture availability, mass transfer, and required energy for the process. In any case, the quality of evapotranspiration estimates is dependent both on the selected model and the quality of the input data.

There is so much literature on evapotranspiration that in this context it is practically impossible to propose even a partial review. Some recent remarkable contributions are due to Zhang et al. (2018); Anapalli et al. (2018); Pozníková et al. (2018); Rongfan et al. (2018); Tang et al. (2018); Negm et al. (2018); Valipour et al. (2017); Fisher et al. (2017); Wang et al. (2017); Feng et al. (2017a,b).

The aim of this paper is to compare actual evapotranspiration estimation models based on advanced models derived from Artificial Intelligence theories. Support Vector Machines, Regression Trees and Ensemble Methods and have been increasingly used in addressing hydraulic engineering problems.

Support Vector Machines (SVMs) have been used in rainfall-runoff modelling (Dibike et al., 2001; Granata et al., 2016). Ahmad et al. (2010) employed SVMs to estimate soil moisture by utilizing remote sensing data. Granata et al. (2017) applied Support Vector Regression (SVR) and Regression Trees in order to predict wastewater quality indicators in urban catchments.

Tree models were used to evaluate sediment transport (Najafzadeh et al., 2017), to predict flood (Solomatine and Xue, 2004), to make predictions of mean annual flood (Singh et al., 2010), to estimate scour depth due to waves (Etemad-Shahidi and Ghaemi, 2011), to forecast sediment yield in rivers (Goyal, 2014). Ensemble methods were employed to tackle wastewater hydraulics problems (Granata and de Marinis, 2017).

Further examples of relevant applications of machine learning techniques to hydrological prediction problems are provided by the works of Wu and Chau (2011); Wang et al. (2013); Taormina et al. (2015); Chau (2017); Fotovatikhah et al. (2018); Granata et al. (2018); Yaseen et al. (2019).

Machine learning algorithms have already been used in evapotranspiration research. Torres et al. (2011) applied Multivariate Relevance Vector Machine and Multilayer Perceptron to forecast ET_o in Central Utah. Shrestha and Shukla (2015) proposed a Support Vector Machine model for the estimation of crop evapotranspiration and crop coefficient. Patil and Deka (2016) used an improved extreme learning machine (ELM) algorithm to estimate weekly reference crop evapotranspiration in the Thar Desert, India. Feng et al. (2017a,b) developed two artificial intelligence models for daily ET_0 estimation only with temperature data, including extreme learning machine (ELM) and generalized regression neural network (GRNN), in 6 meteorological stations of Sichuan basin, China. Nema et al. (2017) investigated the abilities of artificial neural networks (ANN) to improve the accuracy of monthly evaporation estimation in sub-humid climatic region of Dehradun. Tang et al. (2018) employed support vector machine (SVM) and artificial neural network optimized by genetic algorithm, in modeling ET_a in a rainfed maize field under non-mulching and partial plastic film mulching. Mehdizadeh (2018) used multivariate adaptive regression splines (MARS) and gene expression programming (GEP) for estimating daily ET_0, starting from daily weather data of six stations with different climates in Iran. Dou and Yang (2018) used four different machine learning approaches, based on extreme learning machine (ELM), adaptive neuro-fuzzy inference system (ANFIS), artificial neural network and support vector machine, to estimate ET_0 in four different ecosystems. Xu et al. (2018) employed different machine learning approaches for upscaling evapotranspiration from flux towers to regional scale.

However, the applications of machine learning techniques to evapotranspiration estimation problems are currently limited and the knowledge on the topic is still partial and fragmented.

In this study, three different data-driven models were developed for the forecasting of actual evapotranspiration. Models differ in input variables. Four variants of each model were built, changing the applied machine learning algorithm, which are M5P Regression Tree, Bagging, Random Forest and Support Vector Regression. In general terms, no one machine learning algorithm is the best for all problems. The performance of different machine learning algorithms strongly depends on the size and structure of available data. The aforementioned algorithms have been chosen because they usually achieve high performance and they are very good at learning complex, highly non-linear relationships. An effective alternative to the considered algorithms is represented by the Artificial Neural Networks, which have not been used in this study.

The models were trained and tested with data obtained in Central Florida, at an experimental site whose vegetation mainly includes pastures of Bahia grass.

2. Material and methods

2.1. Algorithms

Support Vector Machines (Vapnik, 1995) are supervised learning algorithms able to deal with classification or regression problems. Given a training dataset $\{(x_1, y_1), (x_2, y_2), \ldots, (x_l, y_l)\} \subset X \times R$, where X is the space of the input patterns (e.g. $X = R^n$), Support Vector Regression (SVR) pursues the goal of identifying a function $f(x)$ as flat as possible and with a maximum ε deviation from the experimental target values y_i (Fig. 1a). Hence, given a linear function in the form:

$$f(x) = \langle w, x \rangle + b \tag{1}$$

in which $w \in X$, $b \in R$ and $\langle .,. \rangle$ is the dot product in X, the Euclidean norm $||w||^2$ needs to be minimized, leading to a constrained convex optimization problem.

However, in many cases a certain error has to be accepted. For that reason, slack variables ξ_i, ξ_i^* are introduced in the constraints and the optimization problem is formulated as:

$$\text{minimize} \frac{1}{2} ||w||^2 + C \sum_{i=1}^{l} (\xi_i + \xi_i^*) \tag{2}$$

$$\text{subject to} \begin{matrix} y_i - \langle w, x_i \rangle - b \leq \varepsilon + \xi_i \\ \langle w, x_i \rangle + b - y_i \leq \varepsilon + \xi_i^* \end{matrix} \tag{3}$$

where the constant $C > 0$ affects both the function flatness and the tolerated deviations. The optimization problem may be properly solved in its dual formulation, by means of Lagrange multipliers. The SVR algorithm can be made nonlinear by preliminarily processing the training patterns x_i by means of a function Φ: X→F, where F is some feature space. The SVR algorithm (Fig. 1b) is only depending on the dot products between the different patterns, consequently it is possible to use a kernel $k(x_i, x_j) = \langle \Phi(x_i), \Phi(x_j) \rangle$ instead of explicitly employing the map $\Phi(\cdot)$. The kernel functions commonly used in SVR based models are: linear, polynomial, radial basis function (RBF), and sigmoid. Which one produces the best results depends on the application. In this study, a RBF was selected as kernel. It has the form:

$$k(x_i, x_j) = \exp(-\gamma ||x_i - x_j||^2), \quad \gamma > 0 \tag{4}$$

Preliminary tests have shown that the RBF leads to the best results

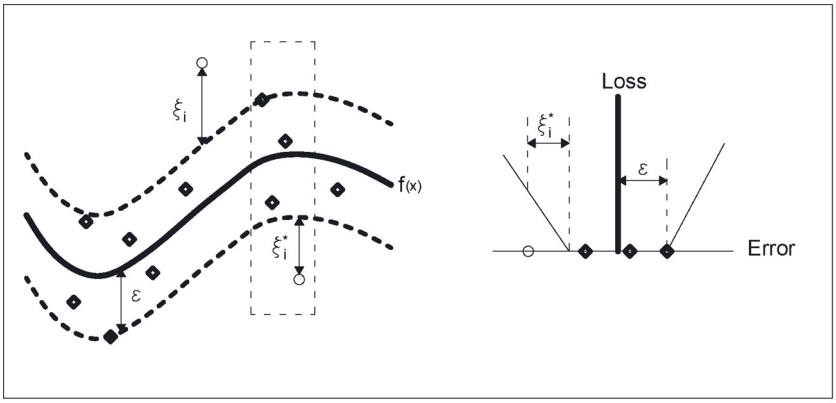

a)

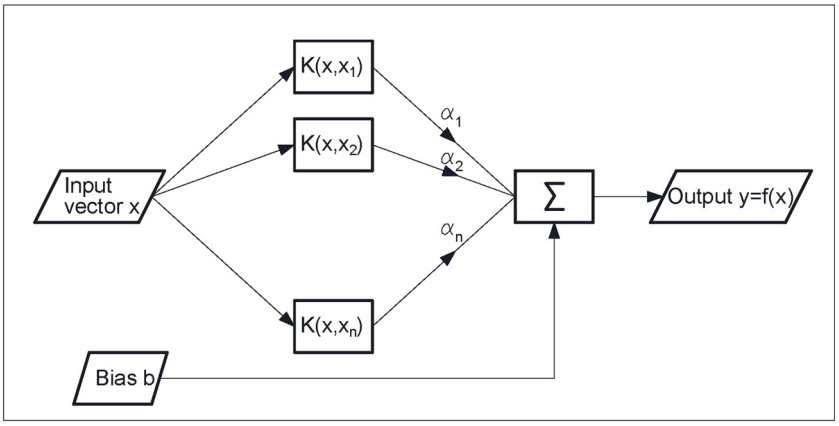

b)

Fig. 1. a) Example of Support Vector Regression. Errors do not matter as long as they are less than ε, while the deviations are penalized; b) Typical architecture of SVR algorithm.

in this specific problem. RBF has advantages of good generalization and strong tolerance to input noise.

A Regression Tree (RT) model (Fig. 2) employs a decision tree as predictive model (Breiman et al., 1984) and the target variables take real values. Internal nodes denote the input variables, whereas leaves correspond to given values of the target variables. Initially, all training data is contained in a root node. The development of a Regression tree model involves the recursive subdivision of the input domain data into subdomains. In each subdomain a multivariable linear regression model is used to make predictions.

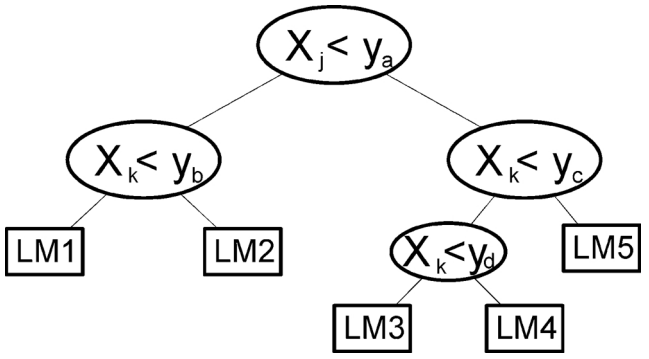

Fig. 2. Typical architecture of Regression tree models. LM are linear models.

The iterative algorithm initially allocates all data into two branches, considering all the potential split on every field. Then, the growth procedure of the regression tree is carried on by splitting each branch into smaller partitions, as the system develops. At each stage the process finds the subdivision in two separate partitions that minimizes the least squared deviation, defined as:

$$R(t) = \frac{1}{N(t)} \sum_{i \in t} (y_i - y_m(t))^2 \quad (5)$$

where $N(t)$ is the number of sample units in the node t, y_i is the value taken by the target variable in the i-th unit and y_m is the mean of the target variable in the node t. This sum evaluates the "impurity" at each node. Indeed, the split process at each node is conducted on the basis of the following function of $R(t)$:

$$\phi(s_p, t) = R(t) - p_L R(t_L) - p_R R(t_R) \quad (6)$$

in which t_L and t_R are the left and right nodes generated by the subdivision s_p, while p_L and p_R are the portions assigned in the left and right child node. Finally, the split s_p that maximizes the value of $\varphi(s_p, t)$ is chosen.

The procedure is repeated until the lowest impurity level is attained or until a stopping rule is met. A stopping rule may depend on the threshold for the minimum impurity variation provided by new splits,

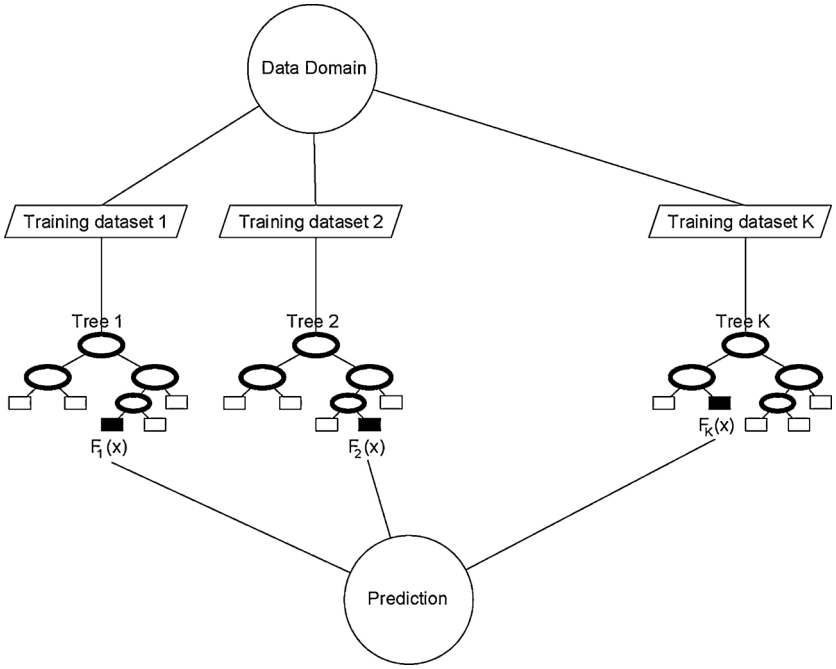

Fig. 3. Typical architecture of Bagging or Random Forest models. The algorithms are different for the way regression trees are built.

the minimum amount of units in each node, or the maximum tree complexity. The algorithm implemented in this study is identified as M5P and arises from Quinlan's M5 algorithm (Quinlan, 1992).

A fully developed Regression Tree model may undergo the problem of overfitting, that occurs when a machine learning model has become too familiar with the data on which it was trained and therefore it is less effective if applied to any other dataset. This risk is generally minimized by means of a pruning process. It reduces the size of the Regression Tree model by removing the splits that do not improve significantly the predicting capability.

A combination of a number of learning models leads to an Ensemble Model. The outputs of different regression tree models are combined into a single result generally using a weighted average. Bootstrap aggregating, better known as Bagging (Breiman, 1996), is one of the most popular ensemble model (Fig. 3). Different training datasets, having the same size, are randomly chosen from the problem domain, without replacement. For each input dataset, a Regression Tree model is built. These trees will be different and will provide different predictions. Small alterations to the training data may lead to significant changes in ramifications and in forecasts for test instances. Bagging allows to obtain a combined model that may outperform the single tree model. Bagging attempts to counteract the instability of the process of regression tree growth by varying the original training dataset instead of sampling a novel training dataset each time: some instances are removed and replaced by others. At last, the single predictions of the regression tree are averaged.

A set of uncorrelated, simple regression trees (Breiman, 2001) also allows to get a Random Forest, one of the most effective ensemble algorithms. Each tree is developed starting from a different bootstrap sample of the data and each new training set is got, with replacement, from the original training set. In addition, Random Forests are different for the way regression trees are built. In a standard tree, each node is allocated referring to the best split among all variables. During the process of development of a Random Forest, instead, at each node a small group of input variables to split on is randomly selected. In the case of M input variables, a number $m < < M$ is identified such that at each node, m variables are randomly chosen out of the M and the best split on these m is used to divide the node. The value of m is kept constant during the growth of the forest. Each tree is expanded as far as possible. No pruning process is carried out.

2.2. Study site

Data are provided by U.S. Geological Survey. They were obtained during a study (Sumner and Jacobs, 2005) performed within a commercial farm located on a sand ridge near Floral City, Florida, USA (Fig. 4). The farm is surrounded by wetlands, a lake and residential areas. The water table was approximately 6–9 m below land surface. The area is characterized by a subtropical humid climate, with a warm wet season lasting from June to September, and a mild dry season lasting from October to May. The average rainfall in the area is over 1300 mm per year. The average annual air temperature is about 21 °C. In winter it rarely falls below 0 °C, while in summer it can exceed 35 °C. Due to the evolution of cloud cover, net solar radiation typically peaks about a month before the start of summer.

Vegetation near the study site mainly includes pastures of Bahia grass (Paspalum notatum Flugge). Grass height averages about 8–12 cm. In the area there are also agricultural fields of strawberries (Fragaria sp.) and brown top millet (Panicum ramosum).

The data were obtained by an Eddy Correlation station and ancillary sensors. The Eddy Correlation technique, also known as Eddy Covariance (Wilson et al., 2001), is a key atmospheric measurement technique to evaluate vertical turbulent fluxes within atmospheric boundary layers. It achieves turbulent flux data by computing the covariance of fluctuations in the vertical wind velocity and in the physical quantity to be evaluated. The detailed characteristics of the measuring instruments can be found in Sumner and Jacobs (2005). The data used in the calculations were collected continuously between 28 September 2000 and 28 September 2004.

3. Results and discussion

The effectiveness of forecasting models was assessed by means of four different criteria: Nash-Sutcliffe model efficiency coefficient (NSE), Mean Absolute Error (MAE), Root Mean Squared Error (RMSE), and Relative Absolute Error (RAE).

The Nash-Sutcliffe efficiency (NSE) is a normalized statistic that determines the relative magnitude of the residual variance compared to

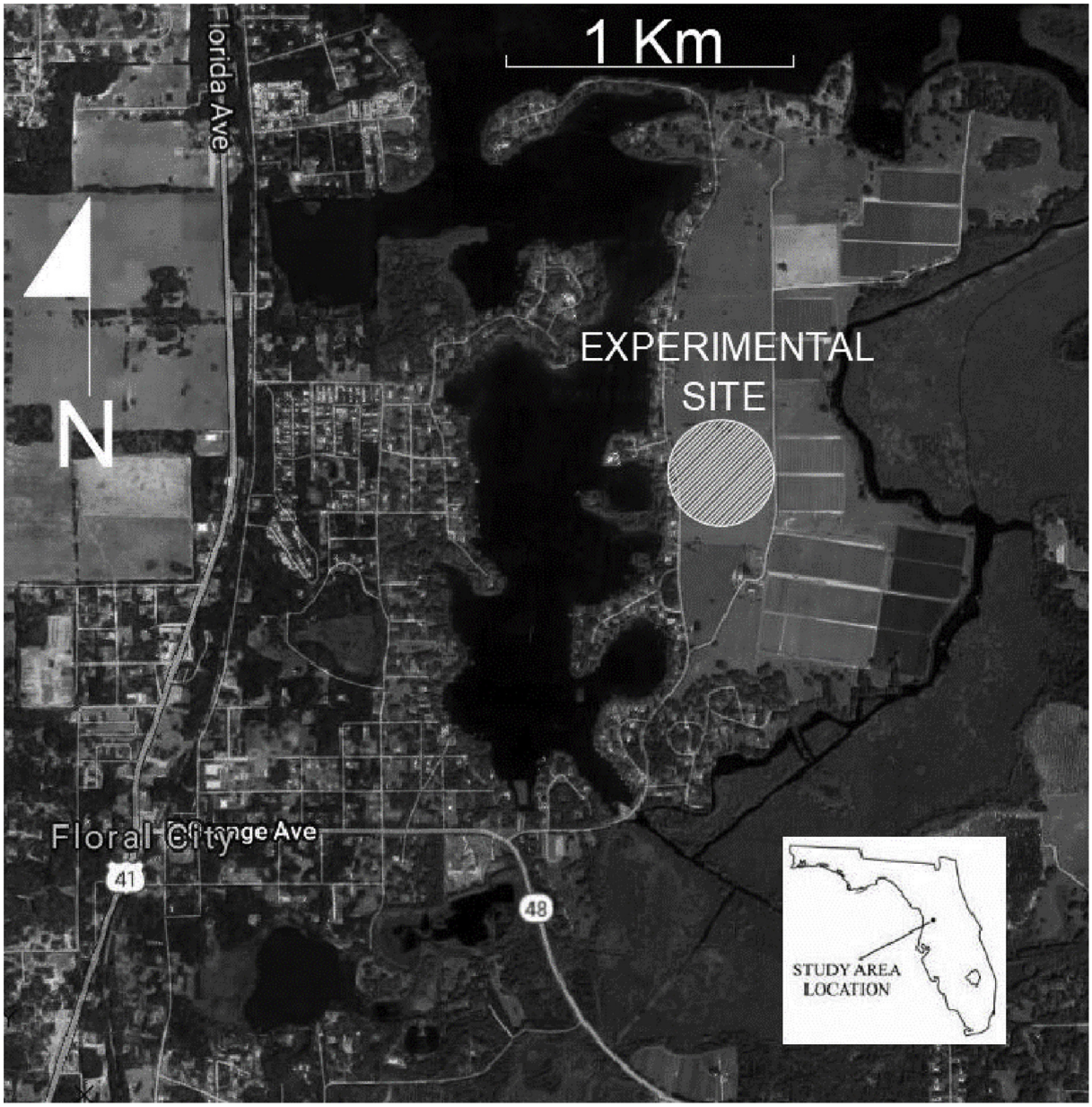

Fig. 4. The study area.

the measured data variance (Nash and Sutcliffe, 1970). It is defined as:

$$NSE = \left(1 - \frac{\sum_{i=1}^{m}(y_i - f_i)^2}{\sum_{i=1}^{m}(y_i - y_a)^2}\right) \quad (7)$$

in which m is the experimental data total number, f_i is the model prediction for data point i, y_i is the experimental value for data point i, y_a is the average of the measured values.

NSE is used to assess the predictive power of the model. It can range from -∞ to 1. Essentially, the closer to 1, the more accurate the model is.

The Mean Absolute Error evaluates the average magnitude of the errors in a set of forecasts, without considering their sign. It's the average over the test sample of the absolute differences between predicted and experimental values. It is defined as:

$$MAE = \frac{\sum_{i=1}^{m}|f_i - y_i|}{m} \quad (8)$$

RMSE is the sample standard deviation of the differences between foreseen and actual values. It is given by:

$$RMSE = \sqrt{\frac{\sum_{i=1}^{m}(f_i - y_i)^2}{m}} \quad (9)$$

Finally, RAE provides a normalized total absolute error according to the following definition:

$$RAE = \frac{\sum_{i=1}^{m}|f_i - y_i|}{\sum_{i=1}^{m}|y_a - y_i|} \quad (10)$$

The four adopted criteria are enough to fully characterize the efficiency of the models. Other evaluation metrics could be used: Median Absolute Percentage Error (MdAPE), Mean Squared Logarithmic Error (MSLE), Fourth Root Mean Quadrupled Error (R4MS4E) and some others (Dawson et al., 2007). MdAPE is less sensitive to the larger errors occurring at high values. R4MS4E is effective in evaluating model goodness of fit on peak and high values. The MSLE, due to the logarithmic transformations involved in its computation, is a good measure for assessing model performances when predicting low values.

However, preliminary tests have shown that different metrics do not alter the comparison, so the use of the adopted, more popular metrics was preferred.

Based on the number of input variables, three different models were obtained for the prediction of ET_a. Four variants of each model were built, varying the implemented machine learning algorithm. Model 1 presents the following daily quantities as input variables: net solar radiation, sensible-heat flux, moisture content of the soil, wind speed, mean relative humidity and mean temperature. Model 2 is characterized instead by the following input variables: net solar radiation, wind speed, mean relative humidity and mean temperature. These variables are essentially the same as the Penman-Monteith model. Finally, Model 3 admits as input variables the net solar radiation, the mean relative humidity and the mean temperature. Model 3 is a simpler model than the others, based only on the most important climatic variables for evapotranspiration estimation. Input variables can be measured with simple and inexpensive instruments practically everywhere, so a similar model has the advantage of being able to be widely used. On the other hand, Model 1 has the advantage of being quite complete with regard to the climatic input variables. Therefore, it should be characterized by greater accuracy, but it can only be used in areas where there are adequate measuring stations. Model 2 has a slightly larger complexity than Model 3 and a slightly smaller applicability.

Each model was developed through a k-fold cross validation process, using a set of 1360 vectors.

In k-fold cross validation, the original dataset is randomly partitioned into k subsets. Then, a single subset is reserved as the validation data for testing the model, while the remaining $k - 1$ subsets are used as training data. The cross validation process is repeated k times: each of the k subsets is used once as the validation dataset. Finally, the k results from the folds are averaged to provide a single estimation. In this study, k was chosen equal to 10. This value ensures satisfactory results.

Table 1 and Figs. 5–16 show the effectiveness of the considered models in the evapotranspiration estimate.

Model 1 shows the best predictive capabilities. All implemented algorithms lead to very high values of NSE (Table 1), greater than 0.98. In particular, M5P is characterized by the highest value of NSE and the lowest error values (NSE = 0.987, MAE = 0.14 mm/day, RMSE = 0.179 mm/day, RAE = 15.4%). The residual plot (Fig. 5b) shows that the highest errors occur in the range 0–2 mm.

The Bagging algorithm, although it provides remarkable results too, is the least effective of the four, showing the lowest value of NSE, equal to 0.98, and the highest error values (MAE = 0.168 mm/day, RMSE = 0.219 mm/day, RAE = 18.5%). Also in this case the residual plot shows that the highest errors occur in the range 0–2 mm. Very similar performances are provided by Random Forest (NSE = 0.981, MAE = 0.167 mm/day, RMSE = 0.218 mm/day, RAE = 18.5%), which leads to the highest errors in the range 0–3 mm (Fig. 6b).

SVR, which is characterized by NSE = 0.983, MAE = 0.153 mm/day, RMSE = 0.201 mm/day, and RAE = 16.9%, shows better performance of both RF and Bagging algorithms.

Model 2 shows less effective forecasting capabilities than Model 1 (Table 1). The values of NSE are appreciably decreased, while the errors are significantly increased. However, the results are still satisfactory. Unlike in the case of Model 1, Random Forest provides best outcomes, showing the highest value of NSE, equal to 0.951, and the lowest errors (MAE = 0.267 mm/day, RMSE = 0.343 mm/day, RAE = 29.3%). SVR in this case is the least performing algorithm (NSE = 0.933, MAE = 0.321 mm/day, RMSE = 0.399 mm/day, RAE = 35.4%), while the forecasting capabilities of M5P (NSE = 0.948, MAE = 0.271 mm/day, RMSE = 0.351 mm/day, RAE = 29.8%) and Bagging (NSE = 0.949, MAE = 0.269 mm/day, RMSE = 0.347 mm/day, RAE = 29.7%) are practically the same. In addition, M5P and Bagging predictors are characterized by an appreciable increase of variance in the results for $ET_a > 3$ mm/day, while SVR shows a clear tendency to underestimate ET_a for values above 3 mm/day.

M5P shows the highest residuals in the ranges 0–1 mm and 2.5–5 mm (Fig. 9b), as well as Bagging (Fig. 10b) and SVR (Fig. 12b). As regards RF (Fig. 11b) maximum residual values are comparable across the whole range of experimental measures

Therefore, not including the sensible-heat flux and the moisture content among the input variables has certain negative consequences on the effectiveness of the predicting model.

Model 3 leads to results that are absolutely comparable with those of Model 2. In some cases, the results obtained by Model 3 are even slightly better than those obtained by Model 2.

Random Forest (NSE = 0.949, MAE = 0.267 mm/day, RMSE = 0.348 mm/day, RAE = 29.4%), M5P (NSE = 0.949, MAE = 0.27 mm/day, RMSE = 0.349 mm/day, RAE = 29.7%) and Bagging (NSE = 0.949, MAE = 0.267 mm/day, RMSE = 0.347 mm/day, RAE = 29.4%) show absolutely equivalent performance. Not even in this case an *ensemble method* can outperform a single regression tree. SVR is the least effective one in predicting actual evapotranspiration (NSE = 0.932, MAE = 0.322 mm/day, RMSE = 0.400 mm/day, RAE = 35.4%).

M5P, Bagging and RF lead to highest residual values for $ET_a > 3$ mm (Figs. 13b, 14 b, 15 b), while SVR shows the highest errors in the ranges 0–1 mm and 3–6 mm. In addition, SVR shows again a clear tendency to underestimate ET_a for values above 3 mm/day.

Table 1
Results of the comparative study.

	Input variables	Machine learning algorithm	NSE	MAE [mm/day]	RMSE [mm/day]	RAE [%]
MODEL 1		M5P Regression Tree	0.987	0.14	0.179	15.4
	Net solar radiation					
	Sensible-heat flux	Bagging	0.98	0.168	0.219	18.5
	Moisture content					
	Wind speed	Random Forest	0.981	0.167	0.218	18.5
	Mean relative humidity					
	Mean temperature	Support Vector Regression	0.983	0.153	0.201	16.9
MODEL 2	Net solar radiation	M5P Regression Tree	0.948	0.271	0.351	29.8
	Wind speed	Bagging	0.949	0.269	0.347	29.7
	Mean relative humidity	Random Forest	0.951	0.267	0.343	29.3
	Mean temperature	Support Vector Regression	0.933	0.321	0.399	35.4
MODEL 3		M5P Regression Tree	0.949	0.27	0.349	29.7
	Net solar radiation					
		Bagging	0.949	0.267	0.347	29.4
	Mean relative humidity					
		Random Forest	0.949	0.267	0.348	29.4
	Mean temperature					
		Support Vector Regression	0.932	0.322	0.400	35.4

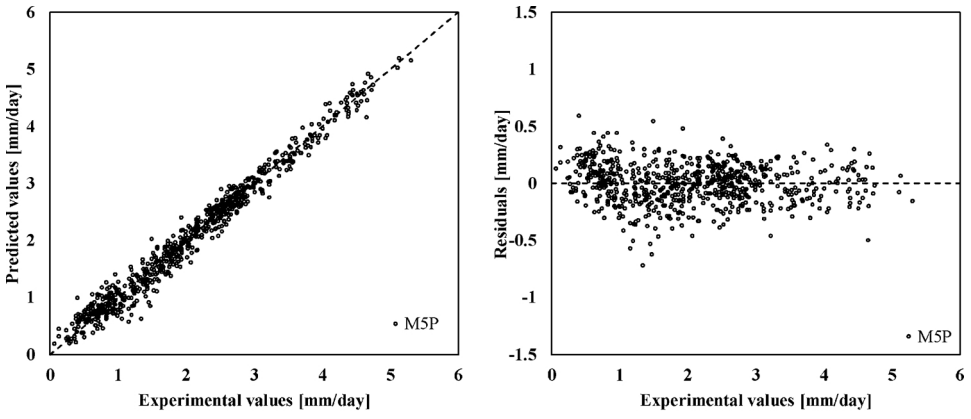

Fig. 5. Evapotranspiration prediction "Model 1" with implementation of the M5P algorithm – a) Predicted versus experimental values, b) Residuals versus experimental values.

A more effective representation of residuals for all models is provided by the notched box plots in Fig. 17. They represent the spread of errors with respect to the experimental values. The lower end of each box plot represents the lower quartile Q1 (25th percentile), the upper end represents the upper quartile Q3 (75th percentile), the band inside the box represents the median of the data. The whiskers extend from the bottom and top of the box to the smallest and highest non-outlier in the dataset.

The blox plots confirm what previously stated on the different accuracy of the developed models. The numerical details are shown in Table 2. It is interesting to note that error distributions are characterized by greater symmetry for SVR-based models, as expected.

Finally, a further comparison among the models can be shown by time series. For the sake of conciseness and readability, Fig. 18 shows the ET_a experimental values and predictions of the different models relating only to about two months, from 29 July 2004 to 28 September 2004. Once again it is possible to detect the greater accuracy of Model 1, but also the very good forecasting capability of both Model 2 and Model 3.

Some relevant findings emerge from the results above shown. The adopted machine learning algorithms are a powerful tool for the prediction of actual evapotranspiration, when a time series of few years is available. In particular, starting from the measurements of a sufficient number of climatic parameters, including the sensible-heat flux and the soil moisture, it is possible to obtain forecasting models characterized by very high accuracy and precision. Sensible-heat flux, as well as net solar radiation, is a major component of the vertical energy balance at the surface. On the other hand, soil moisture dynamics are a central component of the hydrological cycle. Therefore, a data-driven model that takes into account the above two factors most likely leads to satisfactory results.

However, in absence of experimental measurements of sensible-heat flux and moisture content, it is still possible to build a reliable forecasting model of ET_a, with the aid of the machine learning algorithms, based only on mean temperature, net solar radiation and relative humidity data.

This last result is in agreement with the approach proposed by Hargreaves, according to which the evapotranspiration of reference in a given location depends essentially on the temperature, on the extra-terrestrial solar radiation and on appropriate coefficients to be calibrated according to local conditions (Hargreaves and Samani, 1982). These coefficients also take into account the relative humidity and the factors that lead from extra-terrestrial solar radiation to the net solar radiation. The advantage of the approach based on machine learning algorithms is that of directly providing effective evapotranspiration without the need to use crop coefficients

Moreover, the presence of the wind speed among the input parameters does not bring appreciable advantages compared to its absence.

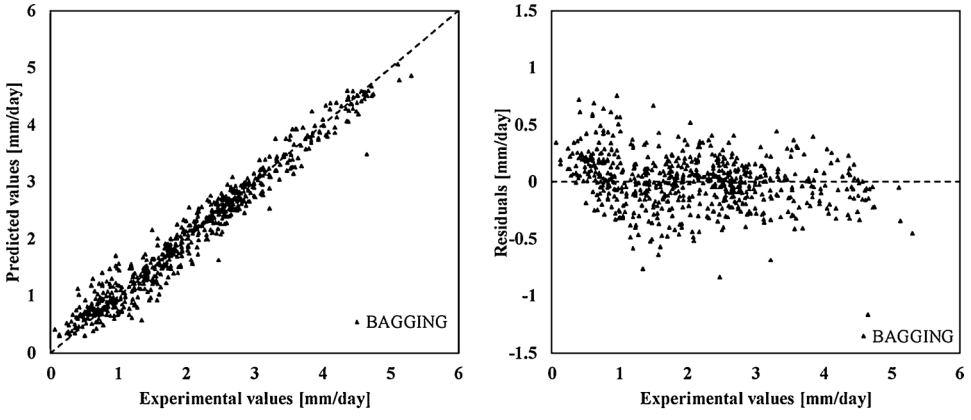

Fig. 6. Evapotranspiration prediction "Model 1" with implementation of the Bagging algorithm – a) Predicted versus experimental values, b) Residuals versus experimental values.

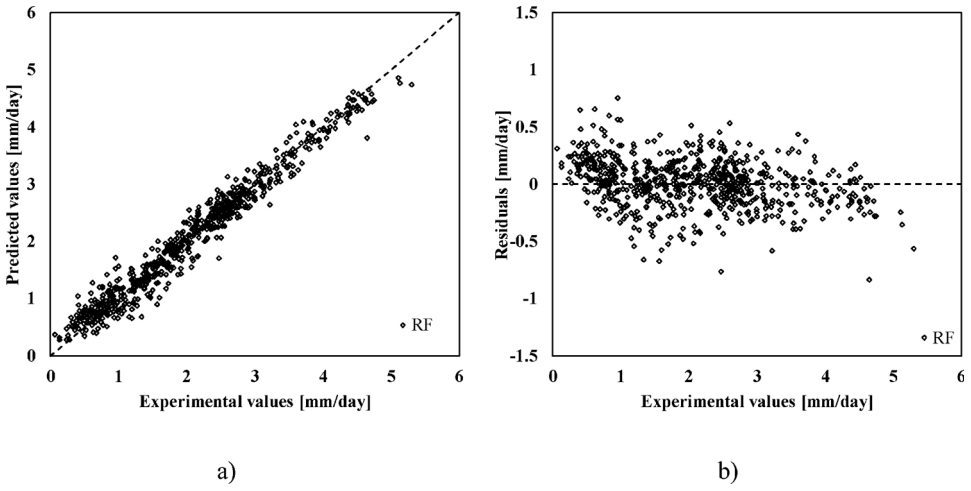

Fig. 7. Evapotranspiration prediction "Model 1" with implementation of the Random Forest algorithm – a) Predicted versus experimental values, b) b) Residuals versus experimental values.

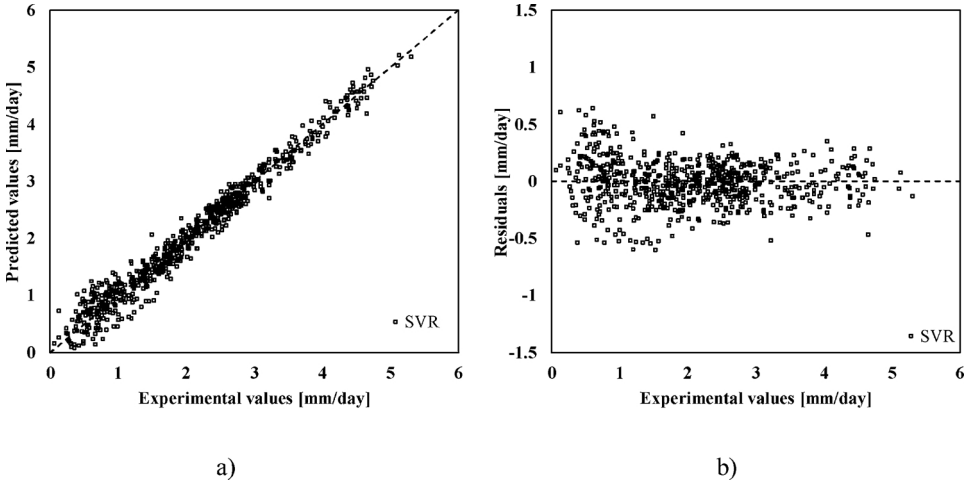

Fig. 8. Evapotranspiration prediction "Model 1" with implementation of the Support Vector Regression algorithm – a) Predicted versus experimental values, b) Residuals versus experimental values.

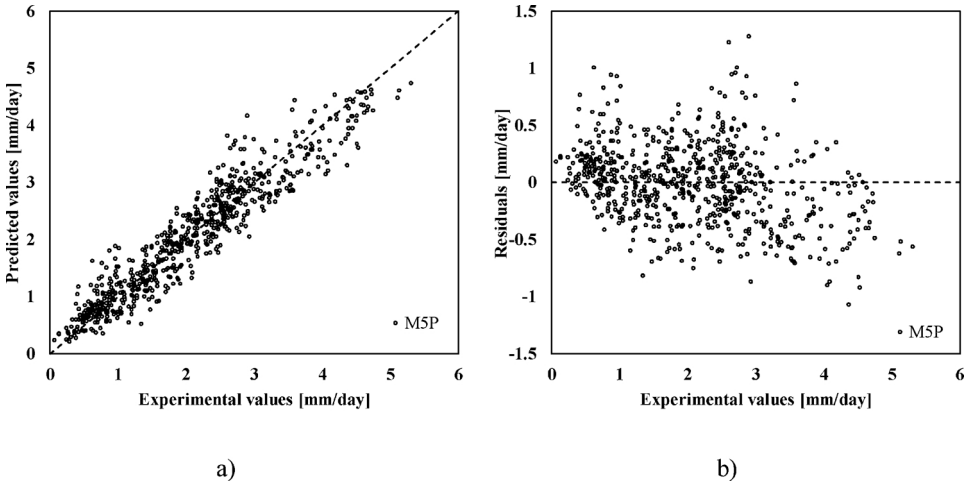

Fig. 9. Evapotranspiration prediction "Model 2" with implementation of the M5P algorithm – a) Predicted versus experimental values, b) Residuals versus experimental values.

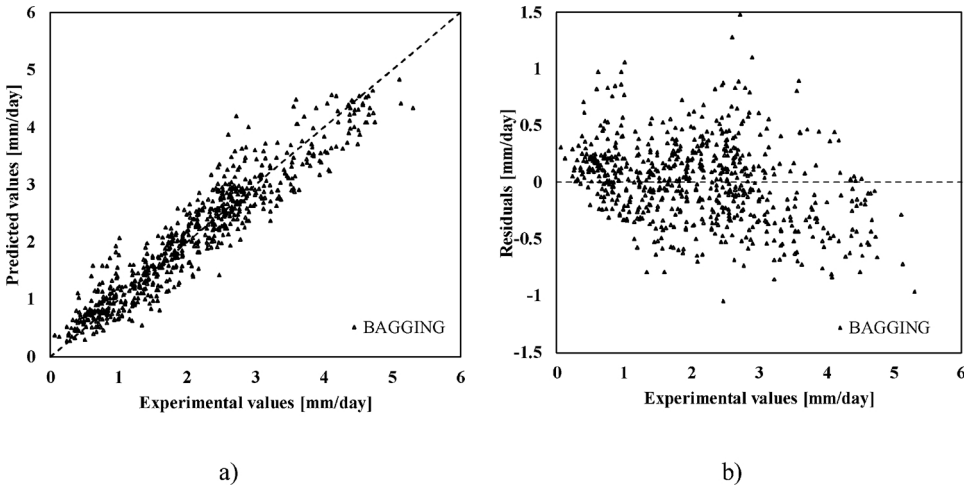

Fig. 10. Evapotranspiration prediction "Model 2" with implementation of the Bagging algorithm – a) Predicted versus experimental values, b) Residuals versus experimental values.

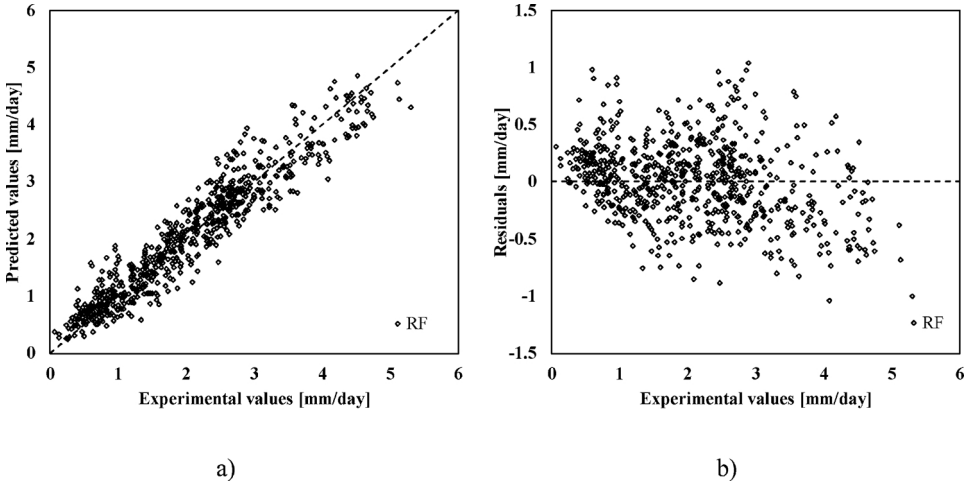

Fig. 11. Evapotranspiration prediction "Model 2" with implementation of the Random Forest algorithm – a) Predicted versus experimental values, b) Residuals versus experimental values.

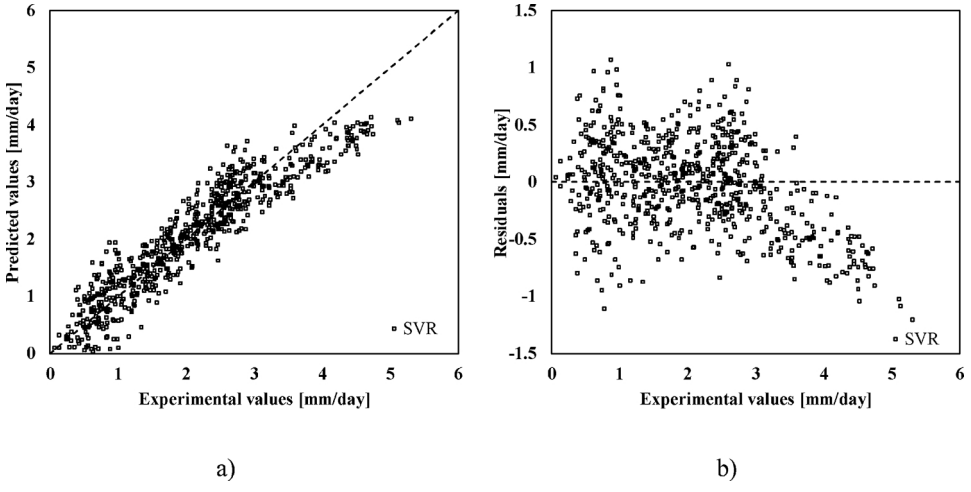

Fig. 12. Evapotranspiration prediction "Model 2" with implementation of the Support Vector Regression algorithm – a) Predicted versus experimental values, b) Residuals versus experimental values.

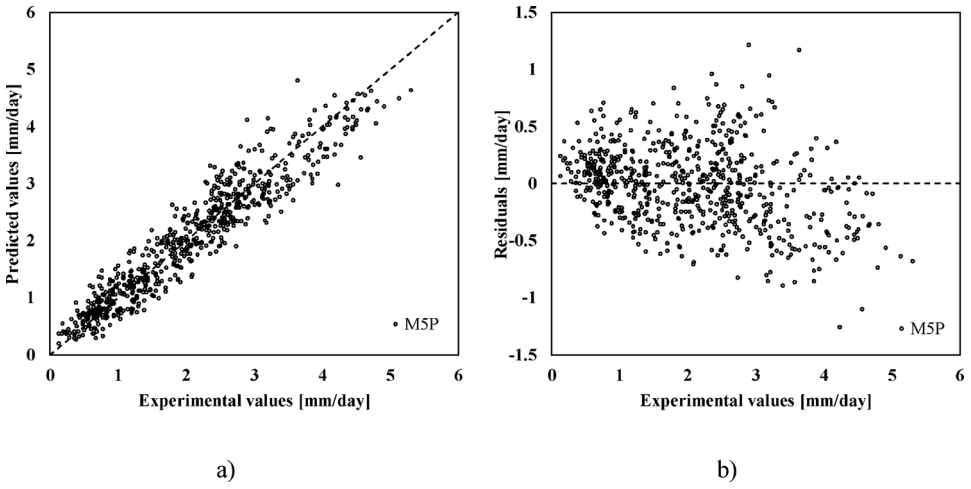

Fig. 13. Evapotranspiration prediction "Model 3" with implementation of the M5P algorithm – a) Predicted versus experimental values, b) Residuals versus experimental values.

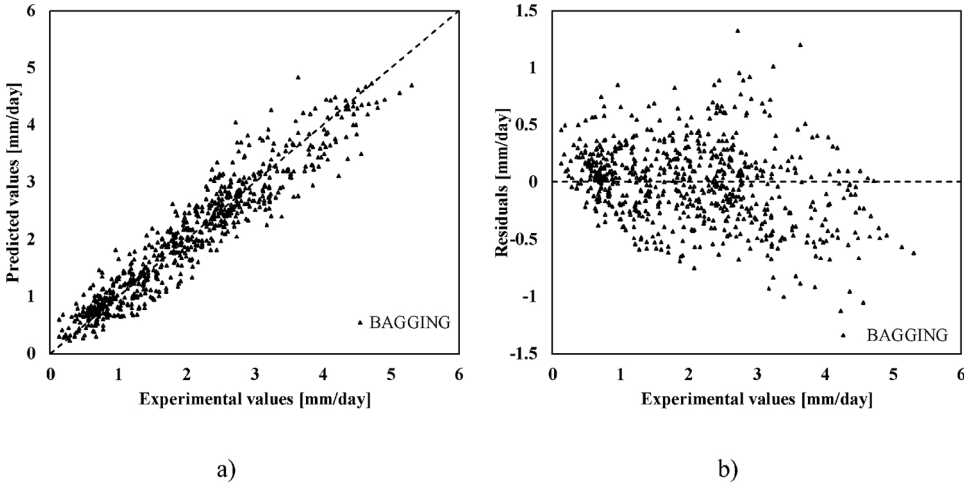

Fig. 14. Evapotranspiration prediction "Model 3" with implementation of the Bagging algorithm – a) Predicted versus experimental values, b) Residuals versus experimental values.

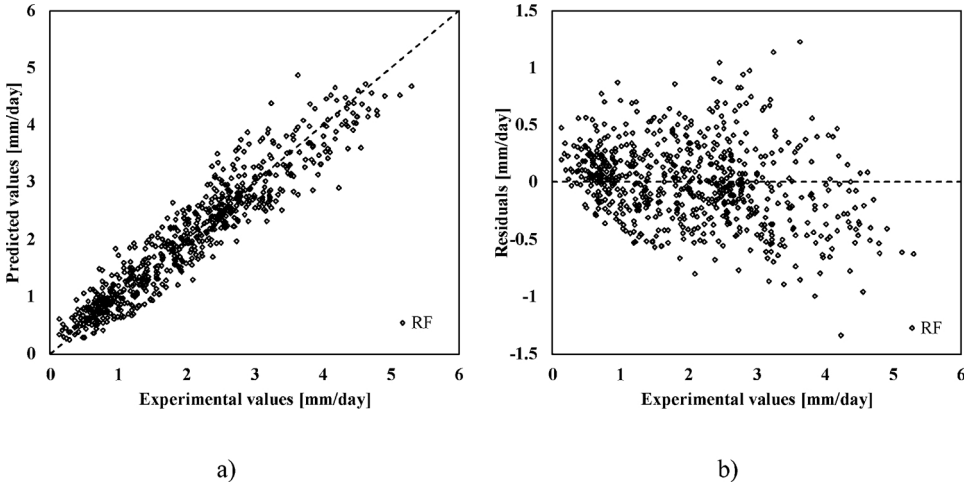

Fig. 15. Evapotranspiration prediction "Model 3" with implementation of the Random Forest algorithm – a) Predicted versus experimental values, b) Residuals versus experimental values.

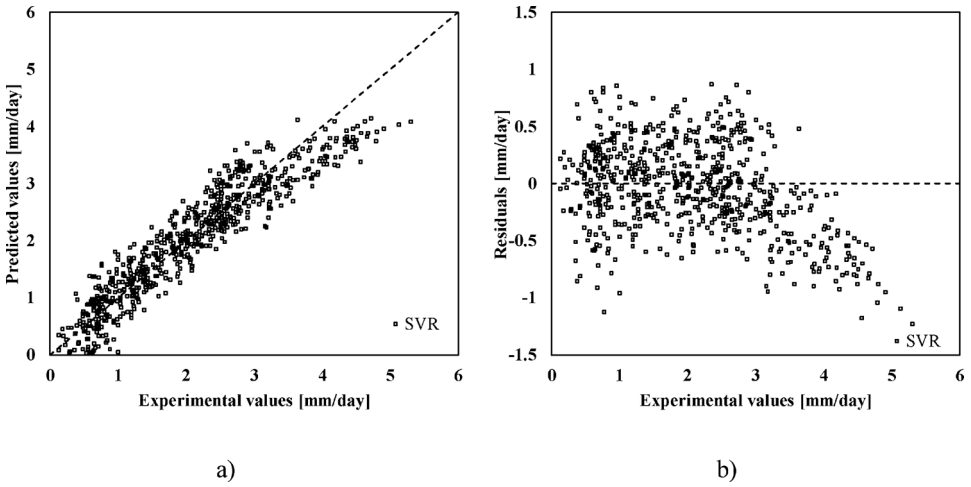

Fig. 16. Evapotranspiration prediction "Model 3" with implementation of the Support Vector Regression algorithm – a) Predicted versus experimental values, b) Residuals versus experimental values.

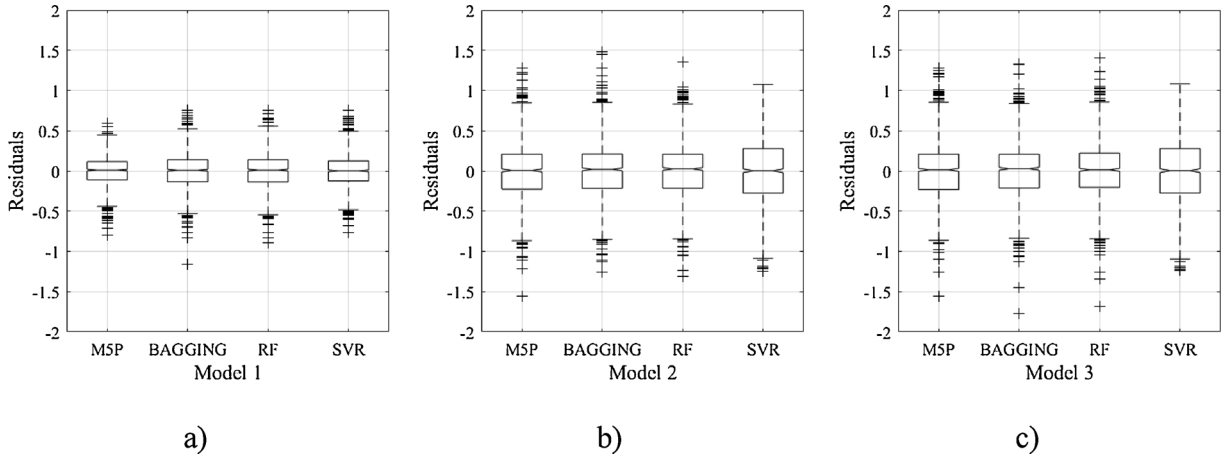

Fig. 17. Box plots of the residuals.

Table 2
Box plots numerical details.

	MODEL 1				MODEL 2				MODEL 3			
	M5P	BAGGING	RF	SVR	M5P	BAGGING	RF	SVR	M5P	BAGGING	RF	SVR
Median	0.01	0.008	0.01	0.001	0.006	0.02	0.025	0.002	0.0135	0.027	0.014	0.0035
25th Percentile	−0.112	−0.1335	−0.137	−0.125	−0.226	−0.217	−0.215	−0.2738	−0.231	−0.213	−0.2045	−0.2725
75th Percentile	0.116	0.14	0.141	0.125	0.209	0.211	0.209	0.278	0.209	0.208	0.2215	0.2785
Minimum	−0.798	−1.162	−0.892	−0.769	−1.556	−1.261	−1.31	−1.251	−1.554	−1.766	−1.686	−1.23
Maximum	0.595	0.753	0.758	0.751	1.28	1.485	1.349	1.075	1.276	1.328	1.404	1.083
Num Outliers	24	24	22	35	28	26	28	6	24	30	29	5

This result is in accordance with the Penman-Monteith approach, which suggests that in the absence of direct measurements of wind speed a constant value of 2 m / s can be assumed.

The use of climatic data that are not very recent may appear to be a limitation of the study. However, projected temperature and precipitation trends in Central Florida appear to be quasi-neutral – with precipitation forecasts more uncertain (Lazarus, 2009). These uncertainties are, in part, related to climate models and their inability to resolve aspects of the global circulation and internal oscillations. However, Florida's recent climate does not seem to have undergone significant changes in either temperature or precipitation.

4. Conclusion

An accurate prediction of actual evapotranspiration is essential for the estimation of irrigation needs and more generally for the careful management of water resources. If experimental data are available, machine learning algorithms represent a powerful tool able to provide accurate predictions.

In this study, three different models were built to predict actual evapotranspiration at a Central Florida site, with a humid subtropical climate. Four variants of each model were built, varying the implemented machine learning algorithm: M5P Regression Tree, Bagging, Random Forest and Support Vector Regression.

Model 1, whose input variables are net solar radiation, sensible-heat flux, moisture content of the soil, wind speed, mean relative humidity

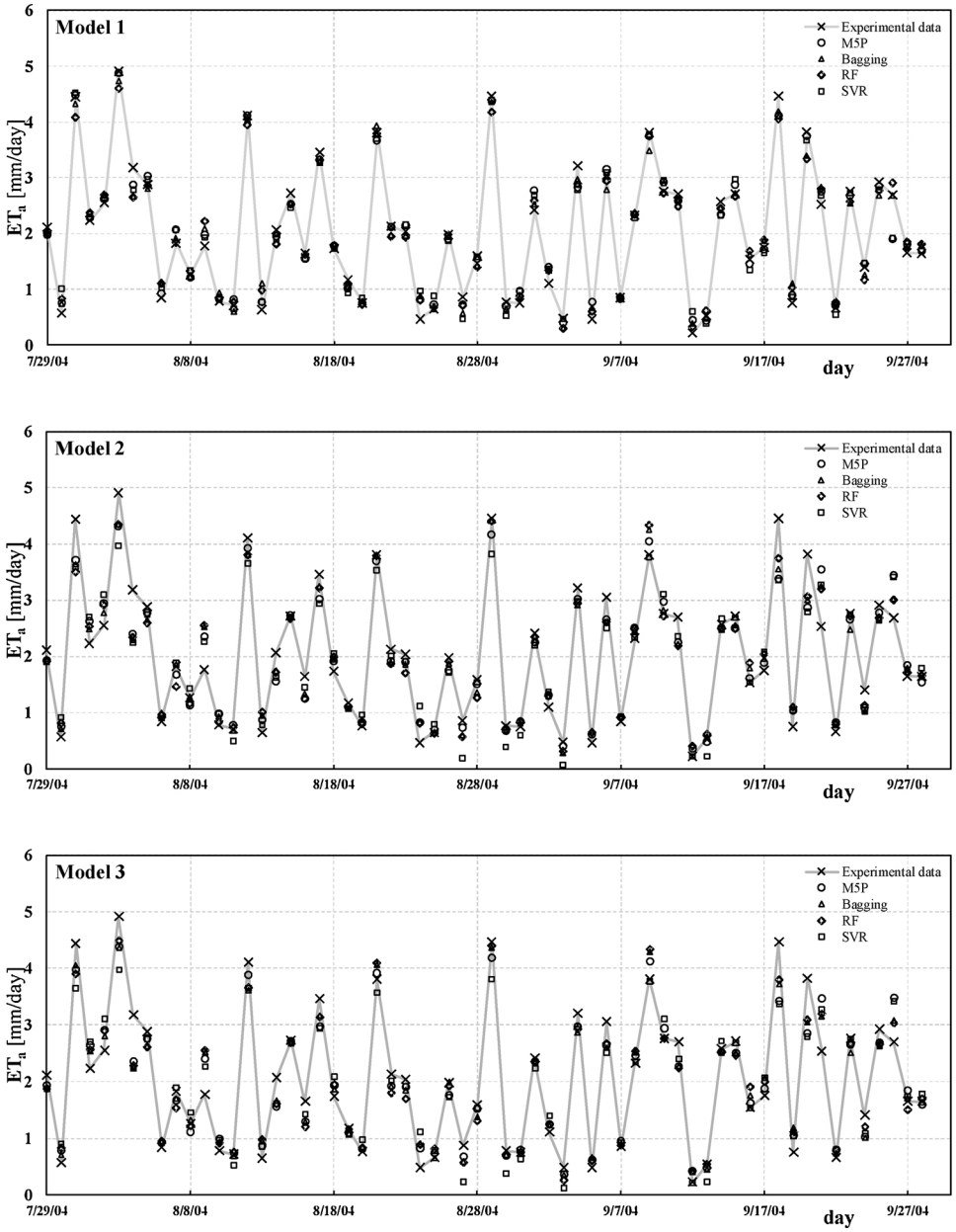

Fig. 18. Comparison by means of time series.

and mean temperature, showed the best predictive capabilities. All the implemented machine learning algorithms provided very good performances. M5P proved to be the most accurate, while RF was the least accurate.

Model 2, whose input variables are net solar radiation, wind speed, mean relative humidity and mean temperature, showed less effective forecasting capabilities than Model 1, but still satisfactory. Unlike in the case of Model 1, Random Forest provided best outcomes, while SVR was the least performing algorithm.

Finally, Model 3, which also excludes wind speed from input variables, led to results that are absolutely comparable with those of Model 2. In this case, Random Forest, M5P, and Bagging show absolutely equivalent performance, while SVR is the least effective algorithm.

Therefore, it is definitely possible to build a reliable machine learning model for predicting actual evapotranspiration starting from mean temperature, net solar radiation and relative humidity data.

The future developments of this study will concern the creation of more complex models, based also on other machine learning algorithms (e.g. ANN, ELM), that contemplate different climatic conditions and that subsequently take into account the effects of climate change, if present.

References

Abtew, W., Melesse, A., 2013. Evaporation and Evapotranspiration. Measurements and Estimations. Springer.

Ahmad, S., Kalra, A., Stephen, H., 2010. Estimating soil moisture using remote sensing data: a machine learning approach. Adv. Water Resour. 33 (1), 69–80. https://doi.org/10.1016/j.advwatres.2009.10.008.

Anapalli, S.S., Fisher, D.K., Reddy, K.N., Wagle, P., Gowda, P.H., Sui, R., 2018. Quantifying soybean evapotranspiration using an eddy covariance approach. Agric. Water Manag. 209, 228–239. https://doi.org/10.1016/j.agwat.2018.07.023.

Breiman, L., 1996. Bagging predictors. Mach. Learn. 24, 123–140. https://doi.org/10.1007/BF00058655.

Breiman, L., 2001. Random forests. Mach. Learn. 45, 5–32. https://doi.org/10.1023/A:1010933404324.

Breiman, L., Friedman, J.H., Olshen, R.A., Stone, C.J., 1984. Classification and Regression Trees. CRC Press.

Chau, K., 2017. Use of meta-heuristic techniques in rainfall-runoff modelling. Water 9 (3), 186.

Dawson, C.W., Abrahart, R.J., See, L.M., 2007. HydroTest: a web-based toolbox of evaluation metrics for the standardised assessment of hydrological forecasts. Environ. Model. Softw. 22 (7), 1034–1052. https://doi.org/10.1016/j.envsoft.2006.06.008.
Dibike, Y.B., Velickov, S., Solomatine, D., Abbott, M.B., 2001. Model induction with support vector machines: introduction and applications. J. Comput. Civ. Eng. 15 (3), 208–216. https://doi.org/10.1061/(ASCE)0887-3801(2001)15:3(208).
Doorenbos, J., Pruitt, W.O., 1977. Crop Water Requirements. FAO Irrigation and Drainage Paper 24, Land and Water Development Division. FAO, Rome.
Dou, X., Yang, Y., 2018. Evapotranspiration estimation using four different machine learning approaches in different terrestrial ecosystems. Comput. Electron. Agric. 148, 95–106. https://doi.org/10.1016/j.compag.2018.03.010.
Etemad-Shahidi, A., Ghaemi, N., 2011. Model tree approach for prediction of pile groups scour due to waves. Ocean Eng. 38 (13), 1522–1527. https://doi.org/10.1016/j.oceaneng.2011.07.012.
Feng, Y., Jia, Y., Cui, N., Zhao, L., Li, C., Gong, D., 2017a. Calibration of Hargreaves model for reference evapotranspiration estimation in Sichuan basin of southwest China. Agric. Water Manag. 181, 1–9. https://doi.org/10.1016/j.agwat.2016.11.010.
Feng, Y., Peng, Y., Cui, N., Gong, D., Zhang, K., 2017b. Modeling reference evapotranspiration using extreme learning machine and generalized regression neural network only with temperature data. Comput. Electron. Agric. 136, 71–78. https://doi.org/10.1016/j.compag.2017.01.027.
Fisher, J.B., Melton, F., Middleton, E., Hain, C., Anderson, M., Allen, R., McCabe, M.F., Hook, S., Baldocchi, D., Townsend, P.A., Kilic, A., Tu, K., Miralles, D.D., Perret, J., Lagouarde, J.P., Waliser, D., Purdy, A.J., French, A., Schimel, D., Famiglietti, J.S., Stephens, G., Wood, E.F., 2017. The future of evapotranspiration: global requirements for ecosystem functioning, carbon and climate feedbacks, agricultural management, and water resources. Water Resour. Res. 53 (4), 2618–2626. https://doi.org/10.1002/2016WR020175.
Fotovatikhah, F., Herrera, M., Shamshirband, S., Chau, K., Faizollahzadeh Ardabili, S., Piran, M.J., 2018. Survey of computational intelligence as basis to big flood management: challenges, research directions and future work. Eng. Appl. Comput. Fluid Mech. 12, 411–437. https://doi.org/10.1080/19942060.2018.1448896.
Goyal, M.K., 2014. Modeling of sediment yield prediction using M5 model tree algorithm and wavelet regression. Water Resour. Manag. 28 (7), 1991–2003. https://doi.org/10.1007/s11269-014-0590-6.
Granata, F., de Marinis, G., 2017. Machine learning methods for wastewater hydraulics. Flow Meas. Instrum. 57, 1–9. https://doi.org/10.1016/j.flowmeasinst.2017.08.004.
Granata, F., Gargano, R., de Marinis, G., 2016. Support vector regression for rainfall-runoff modeling in urban drainage: a comparison with the EPA's storm water management model. Water (Switzerland) 8 (3), 69. https://doi.org/10.3390/w8030069.
Granata, F., Papirio, S., Esposito, G., Gargano, R., de Marinis, G., 2017. Machine learning algorithms for the forecasting of wastewater quality indicators. Water (Switzerland) 9 (2), 105. https://doi.org/10.3390/w9020105.
Granata, F., Saroli, M., de Marinis, G., Gargano, R., 2018. Machine learning models for spring discharge forecasting. Geofluids 13. https://doi.org/10.1155/2018/8328167. 8328167.
Hargreaves, G.H., Samani, Z.A., 1982. Estimating potential evapotranspiration. J. Irrig. Drain. Div. ASCE 108 (1982), 225–230.
Jensen, M.E., 1968. In: In: Kozlowski, T.T. (Ed.), Water Consumption by Agricultural Plants. Water Deficits and Plant Growth, vol. 2. Academic Press, New York, pp. 1–22.
Jensen, M.E., Burmann, R.D., Allen, R.G., 2016. Evaporation and Irrigation Water Requirements, ASCE Manual and Reports on Engineering Practice, vol. 70.
Kool, D., Agam, N., Lazarovitch, N., Heitman, J.L., Sauer, T.J., Ben-Gal, A., 2014. A review of approaches for evapotranspiration partitioning. Agric. For. Meteorol. 184, 56–70. https://doi.org/10.1016/j.agrformet.2013.09.003.
Lazarus, S.M., 2009. Florida's climate: past, present and future. AIP Conf. Proc. 1157 (1).
Mehdizadeh, S., 2018. Estimation of daily reference evapotranspiration (ETo) using artificial intelligence methods: offering a new approach for lagged ETo data-based modeling. J. Hydrol. 559, 794–812. https://doi.org/10.1016/j.jhydrol.2018.02.060.
Najafzadeh, M., Laucelli, D.B., Zahiri, A., 2017. Application of model tree and Evolutionary Polynomial Regression for evaluation of sediment transport in pipes. KSCE J. Civ. Eng. 1–8. https://doi.org/10.1007/s12205-016-1784-7.
Nash, J.E., Sutcliffe, J.V., 1970. River flow forecasting through conceptual models part I – a discussion of principles. J. Hydrol. 10 (3), 282–290. https://doi.org/10.1016/0022-1694(70)90255-6.
Negm, A., Minacapilli, M., Provenzano, G., 2018. Downscaling of American National Aeronautics and Space Administration (NASA) daily air temperature in Sicily, Italy, and effects on crop reference evapotranspiration. Agric. Water Manag. 209, 151–162. https://doi.org/10.1016/j.agwat.2018.07.016.
Nema, M.K., Khare, D., Chandniha, S.K., 2017. Application of artificial intelligence to estimate the reference evapotranspiration in sub-humid Doon valley. Appl. Water Sci. 7, 3903–3910. https://doi.org/10.1007/s13201-017-0543-3.
Patil, A.P., Deka, P.C., 2016. An extreme learning machine approach for modeling evapotranspiration using extrinsic inputs. Comput. Electron. Agric. 121, 385–392. https://doi.org/10.1016/j.compag.2016.01.016.
Pozníková, G., Fischer, M., van Kesteren, B., Orság, M., Hlavinka, P., Žalud, Z., Trnka, M., 2018. Quantifying turbulent energy fluxes and evapotranspiration in agricultural field conditions: a comparison of micrometeorological methods. Agric. Water Manag. 209, 249–263. https://doi.org/10.1016/j.agwat.2018.07.041.
Quinlan, J.R., 1992. Learning with continuous classes. Mach. Learn. 92, 343–348 https://doi.org/10.1.1.34.885.
Rongfan, C., Shanlei, S., Haishan, C., Zhou, S., 2018. Changes in reference evapotranspiration over China during 1960–2012: attributions and relationships with atmospheric circulation. Hydrol. Process. https://doi.org/10.1002/hyp.13252. in press.
Shrestha, N.K., Shukla, S., 2015. Support vector machine based modeling of evapotranspiration using hydro-climatic variables in a sub-tropical environment. Agric. For. Meteorol. 200, 172–184. https://doi.org/10.1016/j.agrformet.2014.09.025.
Singh, K.K., Pal, M., Singh, V.P., 2010. Estimation of mean annual flood in indian catchments using backpropagation neural network and M5 model tree. Water Resour. Manag. 24 (10), 2007–2019. https://doi.org/10.1007/s11269-009-9535-x.
Solomatine, D.P., Xue, Y., 2004. M5 model trees and neural networks: application to flood forecasting in the upper reach of the Huai River in China. J. Hydrol. Eng. 9 (6), 491–501. https://doi.org/10.1061/(ASCE)1084-0699(2004)9:6(491).
Sumner, D.M., Jacobs, J.M., 2005. Utility of Penman-Monteith, Priestley-Taylor, reference evapotranspiration, and pan evaporation methods to estimate pasture evapotranspiration. J. Hydrol. 308 (1), 81–104. https://doi.org/10.1016/j.jhydrol.2004.10.023.
Tang, D., Feng, Y., Gong, D., Hao, W., Cui, N., 2018. Evaluation of artificial intelligence models for actual crop evapotranspiration modeling in mulched and non-mulched maize croplands. Comput. Electron. Agric. 152, 375–384. https://doi.org/10.1016/j.compag.2018.07.029.
Taormina, R., Chau, K.-W., Sivakumar, B., 2015. Neural network river forecasting through baseflow separation and binary-coded swarm optimization. J. Hydrol. 529, 1788–1797. https://doi.org/10.1016/j.jhydrol.2015.08.008.
Torres, A.F., Walker, W.R., McKee, M., 2011. Forecasting daily potential evapotranspiration using machine learning and limited climatic data. Agric. Water Manag. 98 (4), 553–562. https://doi.org/10.1016/j.agwat.2010.10.012.
Valipour, M., Gholami Sefidkouhi, M.A., Raeini－Sarjaz, M., 2017. Selecting the best model to estimate potential evapotranspiration with respect to climate change and magnitudes of extreme events. Agric. Water Manag. 180, 50–60. https://doi.org/10.1016/j.agwat.2016.08.025.
Vapnik, V.N., 1995. The Nature of Statistical Learning Theory. Springer.
Wang, W., Xu, D., Chau, K., Chen, S., 2013. Improved annual rainfall-runoff forecasting using PSO–SVM model based on EEMD. J. Hydroinformatics 15 (4), 1377–1390. https://doi.org/10.2166/hydro.2013.134.
Wang, Z., Xie, P., Lai, C., Chen, X., Wu, X., Zeng, Z., Li, J., 2017. Spatiotemporal variability of reference evapotranspiration and contributing climatic factors in China during 1961–2013. J. Hydrol. 544, 97–108. https://doi.org/10.1016/j.jhydrol.2016.11.021.
Wilson, K.B., Hanson, P.J., Mulholland, P.J., Baldocchi, D.D., Wullschleger, S.D., 2001. A comparison of methods for determining forest evapotranspiration and its components: Sap-flow, soil water budget, eddy covariance and catchment water balance. Agric. For. Meteorol. 106 (2), 153–168. https://doi.org/10.1016/S0168-1923(00)00199-4.
Wu, C.L., Chau, K.W., 2011. Rainfall–runoff modeling using artificial neural network coupled with singular spectrum analysis. J. Hydrol. 399, 394–409. https://doi.org/10.1016/j.jhydrol.2011.01.017.
Xu, T., Guo, Z., Liu, S., He, X., Meng, Y., Xu, Z., Xia, Y., Xiao, J., Zhang, Y., Ma, Y., Song, L., 2018. Evaluating different machine learning methods for upscaling evapotranspiration from flux towers to the regional scale. J. Geophys. Res. Atmos. 123, 8674–8690. https://doi.org/10.1029/2018JD028447.
Yaseen, Z.M., Sulaiman, S.O., Deo, R.C., Chau, K.-W., 2019. An enhanced extreme learning machine model for river flow forecasting: state-of-the-art, practical applications in water resource engineering area and future research direction. J. Hydrol. 569, 387–408. https://doi.org/10.1016/j.jhydrol.2018.11.069.
Zhang, Z., Gong, Y., Wang, Z., 2018. Accessible remote sensing data based reference evapotranspiration estimation modelling. Agric. Water Manag. 210, 59–69. https://doi.org/10.1016/J.AGWAT.2018.07.039.